

---

# 2018

## JOINT INSTITUTE FOR NUCLEAR RESEARCH



### DUBNA

---



# VEKSLER AND BALDIN LABORATORY OF HIGH ENERGY PHYSICS

The activity of the Veksler and Baldin Laboratory of High Energy Physics in 2018 was focused on the implementation and further development of the NICA facility (the Nuclotron–NICA, MPD, BM@N and SPD

projects) and participation in the current research at the Nuclotron as well as in various experiments at world-class accelerator centers.

## MOST IMPORTANT RESULTS IN THE DEVELOPMENT OF THE NICA COMPLEX

Development of the VBLHEP accelerator complex in 2018 was aimed at further construction of the NICA complex systems and elements.

From February to April, the 55th accelerator run at the basic element of the currently developing NICA Complex — the superconducting synchrotron Nuclotron — was performed at extracted ion beams  $^{12}\text{C}^{6+}$ ,  $^{40}\text{Ar}^{16+}$  and  $^{78}\text{Kr}^{26+}$  [1].

Some important results were achieved during the Nuclotron run, in particular:

- For the first time, a nonstructural mode of slow extraction of an accelerated beam from the superconducting synchrotron was implemented using HF noise to improve the quality and uniformity of the bunch (Fig. 1).

- A new source of multicharged ions Krion-6T, which is essential for the heavy-ion program of the

NICA complex, has worked extremely stably and reliably.

- For the first time in Russia, krypton ions with the energy of 3.1 GeV/nucleon were accelerated and extracted from the ring, the possibility of stable operation of the Nuclotron with the field of 18 kG level was demonstrated.

### Nuclotron–NICA Project

#### *Civil Construction*

The western semi-ring of the collider and the electron cooling system placement were prepared for the equipment installation. The construction of the eastern semi-ring is in progress. Status of the MPD Hall preparation complies with the scheduled delivering and positioning the MPD magnet at the end of 2019. The SPD Hall reinforced concrete structure is under

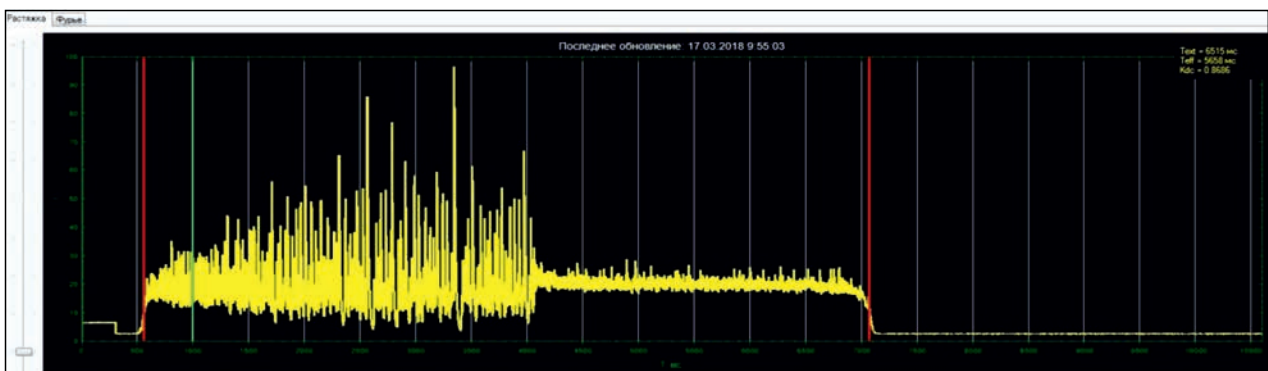


Fig. 1. Left part of the spectrum before kicker switching on; right part — after it

development (80% is ready). The total amount of the mounted reinforced concrete structures is about 500 t.

### ***Booster***

All magnets for the Booster synchrotron were produced and certified. The assembly of the Booster magnetic system was started in September 2018. Two quadrants out of four were equipped with dipole magnets at the end of 2018. Work goes on according to the schedule. Booster commissioning with a beam is expected to be carried out at the end of 2019.

Construction of the beam transport channel from the heavy ion linac (HILac) to the Booster was almost finished. The design of the Booster–Nuclotron beam transporting channel was performed during 2018 in close cooperation with the Budker INP and is in the final stage now. Equipment manufacturing was started.

### ***Collider***

During 2018, work on the design of the beam transporting channels from the Nuclotron to the NICA collider rings was performed under the contract with SigmaPhi Group (France), equipment manufacturing was started.

Fabrication of two RF stations of the system responsible for the injection to the collider is in the final stage. The manufacturing of the collider electron cooling equipment and collider RF stations was also started in 2018. Five dipole collider magnets were produced and successfully tested, 20 yokes for the collider dipole magnets were produced. Pre-serial structural collider magnet was successfully tested, serial production was begun. The production of the high-vacuum beam chambers for the collider magnets was started.

### ***NICA Computing Infrastructure***

The work on the NICA computing infrastructure goes on in close cooperation with JINR LIT. In the scope of this activity, a high-speed network (400 Gb/s) between LIT and VBLHEP was developed and is under commissioning now; a new computer cluster with 4 PB disc space and 4000 CPU cores was put into operation at VBLHEP.

### ***MPD Setup***

#### ***MPD Magnet***

Work on the construction of the superconducting (SC) magnet for the Multi-Purpose Detector (MPD) goes on according to the schedule under the contract signed with ASG Superconductors S. p. A. (Italy) and Vitkovice HM (the Czech Republic). In particular, in 2018 magnet yoke control assembly was successfully performed at Vitkovice HM; magnet cryostat was manufactured and tested; all three modules of the SC coils were produced; the coil is under assembly now; nitrogen screen was manufactured and now is ready for installation; SC magnet power supply system was produced and is ready for the delivery to JINR.

Under cooperation with CERN, a machine for the precise measurement of the magnetic field map in the TPC location area (design parameters:  $8 \cdot 10^3$  points through the area of 814 mm in diameter with the length of 3400 mm along the magnet axes) was produced and will be delivered from CERN to JINR in 2019.

### ***Time Projection Chamber***

Time projection chamber (TPC) is the main element of the MPD tracking and particle identification systems. The following works were performed on the TPC in 2018: the clean room for TPC assembly and corresponding equipment were established; all main elements of the detector body were delivered to JINR and are ready for assembly; the TPC HV electrode was manufactured; the pilot system including 512 channels for the TPC front-end (FE) electronics based on the SAMPA chips was produced and successfully tested; the geometry of the TPC read-out chamber frame boxes was tested; the development of the LV power supply was going on in collaboration with BSU (Minsk); two lasers for the TPC alignment were put into operation; commissioning of the TPC gas system was started and is in progress now.

### ***Time of Flight (TOF) System***

In 2018, mass production of the MPD TOF system was started, frame boxes for the detectors and electronics for the TOF are ready; manufacturing of the detectors goes on. Base components of the TOF gas system were produced by the team from the Warsaw University of Technology.

### ***Fast Forward Detector (FFD)***

In 2018, the following results on the FFD system were achieved:

- The design of the detector and FE electronics installation around the beam pipe was prepared.
- HV power supply system based on the modules of Wiener and Iseg was designed.
- Electronics of FFD and trigger were developed and prototyped.
- The test bench for FFD modules with cosmic muons was assembled.
- Laser alignment system project was finalized; system tests were started.

### ***Electromagnetic Calorimeter***

One of the unique high-tech subsystems of the MPD experiment is the large-scale shashlyk-type electromagnetic calorimeter with projection geometry. It is required to produce more than 40 thousand modules and assemble them into a single cylindrical system, calibrate them and put into operation. This is a joint project with Tsinghua University (Beijing). The following results were achieved:

- The production of all components of the electromagnetic calorimeter was established. Almost 50% of

scintillation plates (out of  $10^7$ ) and bearing plates (out of  $3 \cdot 10^4$ ) were produced at two plants. The order on the manufacturing of the lead plates ( $10^7$  units) was placed on two plants.

- Two sections of the calorimeter module assembly were organized at IHEP and Tensor plant (Russia). They cover the JINR share (25%). The site for the modules assembly of the China share (75%) was organized in Beijing as well. The issue of funding is still open.

- First produced modules were successfully tested.
- Works on the design of the MPD power structure were performed in Khotkovo (Moscow Region), the first samples are expected to be ready at the end of 2019.

### BM@N Setup

BM@N setup is under permanent extending. In 2018, the central tracker was equipped with three forward Si strip detectors and six GEM detectors  $163 \times 45$  cm. During the data taking, two types of TOF detectors, electromagnetic and hadron calorimeters, outer tracker, including drift tube planes and cathode strip chamber, detector for the neutron registration, beam monitoring and trigger detectors were used.

Last year, the BM@N physics program was extended by “Probing Short-Range Correlations” (SRC). An international team, which includes physicists from JINR, Russia, USA, Germany, France and Israel, prepared the setup and provided the first data taking on this program during the 55th Nuclotron run. Almost 20 TB (8M events) of data with 4-GeV carbon ion beam and liquid hydrogen target were obtained. Data analysis is in progress.

After the SRC run, the equipment was rearranged for the BM@N heavy ion program, and the run was continued with argon and krypton beams with kinetic energy of 3.2 and 2.3 (2.9) GeV, respectively. The measurements were aimed at the detection of inelastic interactions of ion beams with nuclear targets (Al, Cu, Sn, Pb) to study production of hyperons, strange mesons, light nucleus fragments, and multigamma states. Obtained statistics composes 200M events. Data analysis is in progress [2].

### MPD and BM@N Common Issues

Two “kick off” meetings were organized in April and October 2018 to form the BM@N and MPD collaborations.

The discussions and presentations at the first meeting were centered around three main topics:

- current status and plans for the MPD and BM@N experiments, including all subsystems, simulations, expected performance of the detectors and preparedness for data analysis;
- current status and schedule of the NICA facility including the expected machine parameters;

- procedures to establish and adopt the by-laws of the collaborations, including the formation of the governing bodies of the collaborations.

The major aim of the second meeting was to discuss the present state and work plans for the MPD and BM@N experiments and elections of governing bodies of the collaborations. M. Kapishin was elected a BM@N spokesman and A. Maksimchuk — a BM@N technical coordinator; A. Kisel was elected a spokesman of the MPD, and V. Golovatiuk becomes an MPD technical coordinator. The BM@N collaboration was formed by 216 participants from 17 institutions presented by 10 countries; MPD, by 436 participants from 26 institutions and 10 countries.

The Protocol to the Cooperation Agreement between the European Organization for Nuclear Research (CERN) and the Joint Institute for Nuclear Research (JINR) concerning the development and provision by CERN of monolithic pixel detectors, TPC front-end electronics, and other items for the MPD experiment at the NICA facility at JINR was signed in 2018.

### Silicon Vertex Detector

In 2018, the works on a wide-aperture silicon tracking system (STS) of the BM@N facility were continued. Production line for the STS modules assembly on layouts was fully debugged, and the works on the assembly of working modules were started.

In December 2018, a test run on the extracted electron beam with the energy of 100 MeV at the Linac-200 (JINR) was held. During the run, the operation of the electronics for the STS of the experiment was tested. The setup consisted of two test stations based on double-sided micro-strip silicon sensors measuring  $1.5 \times 1.5$  cm. The thickness of the sensors is  $300 \mu\text{m}$ , the width of the strips is  $58 \mu\text{m}$ , the angle between the strips is  $90^\circ$ . The signal was read out and processed using STSXYTER v.2.0 and subsequent AFCK and FLIB blocks based on FPGA modules. As a result of the run,  $\sim 200$  GB of data for electron energies from 50 to 100 MeV were collected. Based on the data obtained, the following parameters are to be investigated: cluster sizes that depend on energy, charge collection efficiency, and signal-to-noise ratio.

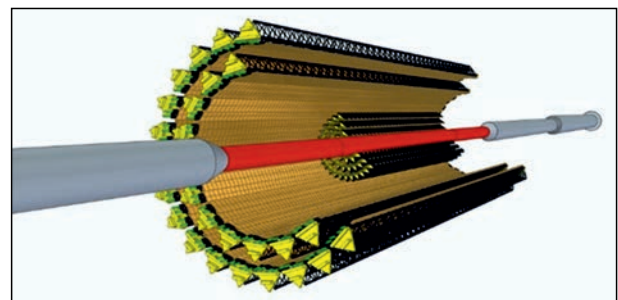


Fig. 2. 3D image of a five-layer tracker for MPD of the “optimal” variant

The run was performed in cooperation with a group from St. Petersburg State University (under the leadership of V. Zhrebchevsky), which performed the study of monolithic active pixel sensors ALPIDE. These sensors will be used to develop the internal tracker of the NICA-MPD facility.

Within the project on the development of an internal tracking system of MPD-ITS, the preliminary design of the tracker was carried out (Fig. 2). A design of the facility with a thin-walled beryllium ion pipeline and related devices in the TPC zone was developed.

### SPD Setup

The proposed SPD detector is aimed at implementation of the scientific program presented in LOI, supported by the PAC for Particle Physics in 2014, and should meet the following requirements:

- close to  $4\pi$  geometrical acceptance;
- high-precision ( $\sim 50 \mu\text{m}$ ) and fast vertex detector;
- high-precision ( $\sim 100 \mu\text{m}$ ) and fast tracker;
- good particle ID capabilities;
- efficient muon range system;
- good electromagnetic calorimeter;
- low material budget over the track paths;
- trigger and DAQ system able to cope with event rates at luminosity of  $10^{32} \text{ (cm} \cdot \text{s)}^{-1}$ ;
- modularity and easy access to the detector elements, that makes further reconfiguration and upgrade of the facility possible.

In 2018, an official project “Conceptual and Technical Design of the Spin Physics Detector (SPD) at the NICA Collider” [3] was prepared to be presented for the approval at the 50th PAC for Particle Physics.

## EXPERIMENTS CARRIED OUT AT THE NUCLOTRON

### FASA

The kinetic energy spectra of intermediate mass fragments ( $2 < Z < 20$ ) have been studied for the data obtained by the group in 4.4 GeV  $d + \text{Au}$  collisions [4]. An example of kinetic energy spectra for boron and neon fragments is shown in Fig. 3. The strong difference between the experimental data and calculated ones in the framework of the intranuclear cascade (INC) and statistical multifragmentation model (SMM), which in-

cludes no flow, is seen. It was suggested that this enhancement is caused by the expansion of the system, which is assumed to be radial. SMM gives the coordinates  $R_Z$  and momenta of the fragments with charge  $Z$  in the freeze out volume with radius  $R_{\text{sys}}$ . To describe the experimental data, the radial velocity for each particle in freeze out volume was added. A homogeneous radial expansion was assumed, in which the flow velocity is a linear function of the particle from the center of mass. The velocity  $V_{\text{flow}}(Z)$  of a particle with

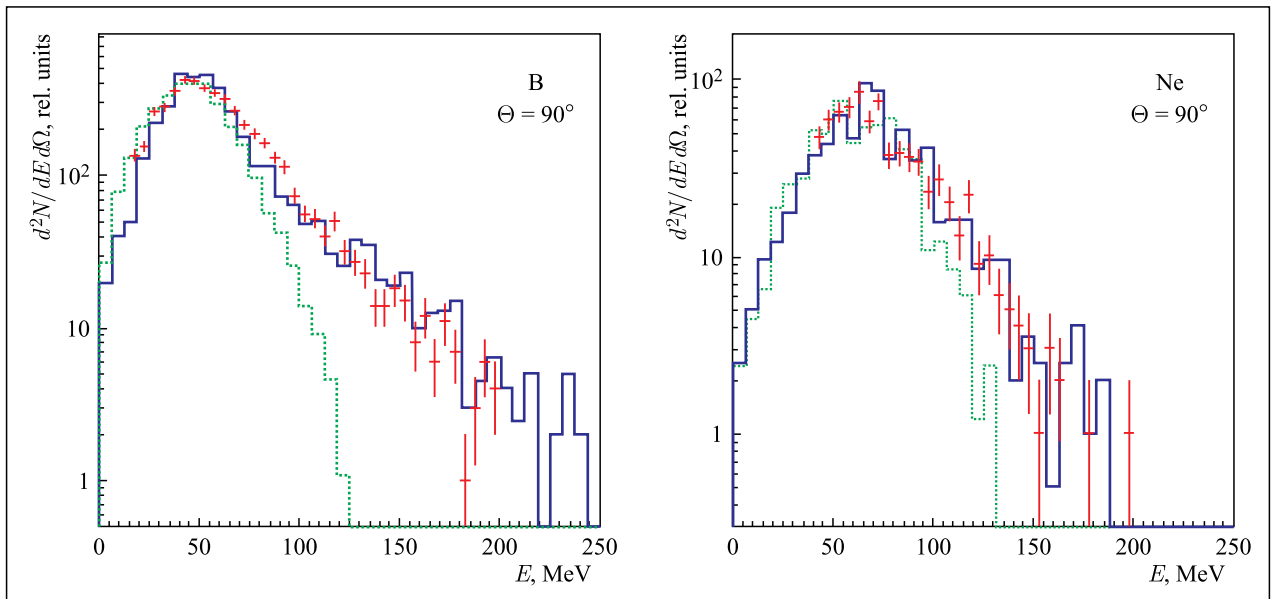


Fig. 3. Kinetic energy distributions of boron and neon fragments obtained for  $d$  (4.4 GeV) + Au collisions at polar angle  $\Theta = 90^\circ$ . Points are experimental data. Solid lines (blue): INC + SMM calculations with radial flow  $V_{\text{flow}}^0 = 0.15c$  ( $c$  — light speed) for boron distribution and  $V_{\text{flow}}^0 = 0.08c$  for neon distribution. Dotted lines (green): INC + SMM calculations without radial flow

a charge  $Z$  located on a radius  $R_Z$  was taken as follows:

$$V_{\text{flow}}(Z) = V_{\text{flow}}^0 \frac{R_Z}{R_{\text{sys}}},$$

where  $V_{\text{flow}}^0$  is the radial velocity at the surface of the system. The value of  $V_{\text{flow}}^0$  has been adjusted to describe the measured kinetic energy of fragments. A good agreement of measured and calculated kinetic energy spectra including a radial flow was found.

## DSS

Within the DSS project, the following important results were obtained in 2018:

- An upgraded version of the experimental facility on the internal beam for measuring short-range nucleon–nucleon correlations in the interaction of light nuclei was fully put into operation during the 55th run of the Nuclotron.

- Analysis of experimental data on the angular dependence of the elastic  $d-p$  scattering cross section at the deuteron energies of 1000, 1300 and 1800 MeV obtained at the internal target was performed.

- Analysis of experimental data on the angular dependences of the deuteron analyzing powers  $A_x$ ,  $A_y$  and  $A_{xx}$  of elastic  $d-p$  scattering at the deuteron energies of 400, 700, 800 and 1000 MeV obtained at the internal target was performed [5].

## PARTICIPATION IN EXPERIMENTS AT EXTERNAL ACCELERATORS

### Experiments at the Large Hadron Collider

#### ALICE

New results of femtoscopic correlation functions for  $K^+K^-$  pair production in Pb–Pb collisions at 2.76 TeV per nucleon pair are presented in Fig. 4. One can see the new Dubna fit (Fig. 4, *a*) within the FSI model using traditional parameters of  $a_0(980)$  (Martin, Achasov) and free ones for  $f_0(980)$  with small coupling constant [6]. The data and model agreement is visibly better than for the fit with all traditional parameters (Fig. 4, *b*). The new value of  $f_0$  width ( $(7.0 \pm 2.2)$  MeV) was obtained from Dubna fit which corresponds to the one of BESIII collaboration ( $(9.5 \pm 1.1)$  MeV).

New results were obtained for comparison of the ALICE femtoscopic data with the EPOS-3 model for

$p$ –Pb collisions at 5.02 TeV [7]. Figure 5, *a* shows that the data and model femtoscopic emission source radii are compatible well at the same centralities but only with including hadronic cascade rescattering mechanism.

New results were obtained with the JINR team participation for the  $J/\psi$  production in ultraperipheral Pb–Pb collisions at 5.02 TeV. The differential cross section is shown in Fig. 5, *b* with the theoretical predictions at different gluon shadowing contributions in nuclei.

The tests of the modules of the PHOS ALICE electromagnetic calorimeter were performed on the beams of electrons at PS and SPS CERN accelerators in the energy range of 1–160 GeV. This study was aimed at making the optimal choice for the upgrade of photodetectors and readout electronics. The goal of the upgrade

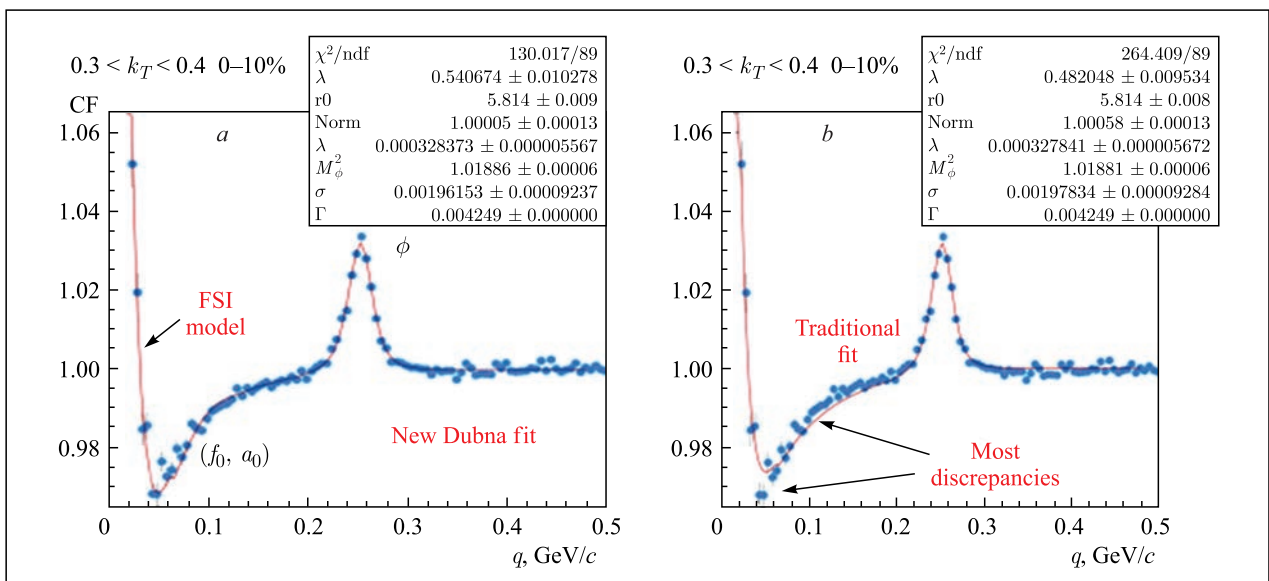


Fig. 4. The femtoscopic correlation functions for  $K^+K^-$  pairs production in Pb–Pb collisions at 2.76 TeV

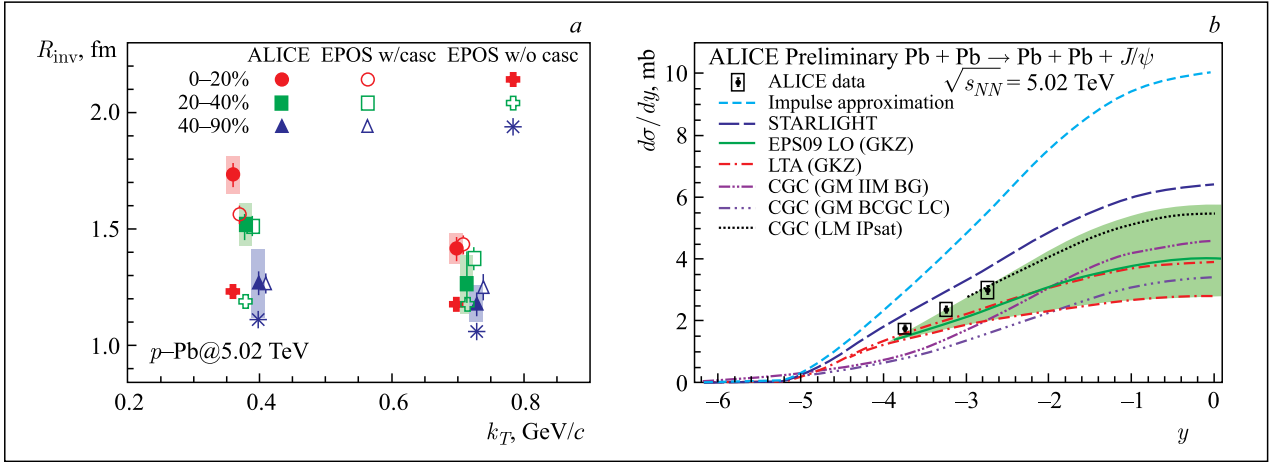


Fig. 5. *a*) Emission source radii of  $K^{\text{ch}}K^{\text{ch}}$  pairs versus pair transverse momentum. *b*) Differential cross section versus rapidity of  $J/\psi$  production in comparison with different model predictions

is to provide the calorimeter functioning at the room temperature without worsening of the energy resolution and with the improvement of the time resolution. Currently, PHOS is running at the temperature of  $-25^\circ\text{C}$  and has the time resolution of  $\sigma_t = 3\text{--}4$  ns. A number of tests performed on the electron beams at CERN with different SiPMs have shown that it is possible to reach the time resolution better 500 ps at working temperature  $T = +18^\circ\text{C}$ .

### ATLAS

In 2018, the ATLAS group members were engaged in the following activities: experimental data analysis, simulation of the new process including SUSY particles, participation in the ATLAS detector upgrade program for high-luminosity environment at HL-LHC as well as QCD analysis of the DIS data.

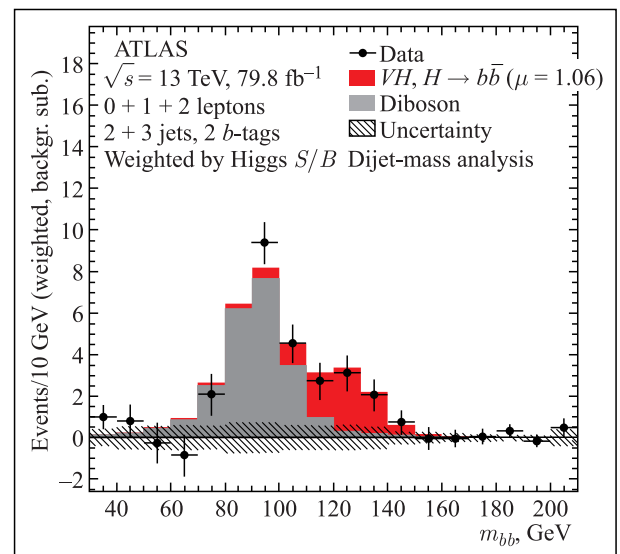
Observation of the Higgs boson decay into a pair of  $b$  quarks, reported at the major international confer-

ence ICHEP2018 in Seoul, was announced in CERN press-release, in communications from the ATLAS collaboration, and in many publications at the scientific centers (including Dubna), as the most significant result of the ATLAS experiment in 2018 [8].

The ATLAS data corresponding to an integrated luminosity of  $79.8 \text{ fb}^{-1}$  of proton-proton collisions collected at a centre-of-mass energy of  $\sqrt{s} = 13 \text{ TeV}$  in Run-2 in 2015–2017 were analyzed. An excess over the expected background was observed, with a significance of 4.9 standard deviations compared with an expectation of  $4.3\sigma$ . The measured signal strength relative to the SM prediction for  $m_H = 125 \text{ GeV}$  was found to be  $\mu = 1.06 \pm 0.16(\text{stat.}) + 0.21 - 0.19(\text{syst.})$ . The invariant mass spectrum of two  $b$  jets is presented in Fig. 6.

ATLAS has already observed all four main production modes of the Higgs boson, two of which this year. These observations mark a new milestone in the study

Fig. 6. The distribution of  $m_{bb}$  in data after subtraction of all backgrounds except for the  $WZ$  and  $ZZ$  diboson processes, as obtained with the dijet-mass analysis. The contributions from all lepton channels,  $p_T^V$  regions and number-of-jets categories are summed and weighted by their respective  $S/B$ , with  $S$  being the total fitted signal and  $B$  the total fitted background in each region. The expected contribution of the associated  $WH$  and  $ZH$  production of a SM Higgs boson with  $m_H = 125 \text{ GeV}$  is shown scaled by the measured signal strength ( $\mu = 1.06$ ). The size of the combined statistical and systematic uncertainties for the fitted background is indicated by the hatched band



of the Higgs boson, as ATLAS transitions from observations to precise measurements of its properties. Precision analysis of the  $H \rightarrow b\bar{b}$  decay for the Higgs boson produced in association with the vector boson  $W/Z$  is also promising for searches for the new physics beyond the Standard Model.

### CMS

In 2018, the JINR group took part in data taking, processing and physics analysis of data collected during the LHC Run-2 with the proton beams at energy of 13 TeV and luminosity up to  $2.32 \cdot 10^{34} \text{ sm}^{-2} \cdot \text{s}^{-1}$ . Figure 7 shows the result on the search for new neutral resonances (both with spin 1 and spin 2) in expected decays to muon pairs. The model-independent 95% CL upper limits on cross sections of these processes were measured, as well as the 95% CL mass limits for these resonance states were set (Fig. 8). The new mass limits are 4.5 and 3.7 TeV for the sequential standard model (SSM) and the  $\psi$  model of  $E_6$  GUT, respectively; for the Randall–Sundrum model with the coupling  $c = 0.01–0.1$ , masses less than 2.00–4.01 TeV are excluded; for a simplified dark matter model with the exchange of a mediator particle in the  $s$ -channel, the mediator mass is excluded for less than 1.8 and 4 TeV, for vector and axial-vector coupling constants, respectively [9]. Moreover, the results on the dependence of the muon momentum resolution on the momentum using two muon tracks produced by cosmic muons were obtained [10].

In 2018, the analysis of the high-multiplicity events (leptons, photons, and jets with  $p_T > 50 \text{ GeV}/c$ ) was

completed with the first Run-2 data ( $L_{\text{int}} = 35.9 \text{ fb}^{-1}$ ). The model-independent 95% CL limits on the product of the cross section and the acceptance of a new physics signal in these final states are set for the different categories of events with multiplicity  $N \geq 11$  and for the  $S_T$  value of 1.5–8.0 TeV. Semiclassical black holes and string balls with masses as high as 7.2–10.2 TeV are excluded for the value of the fundamental Planck mass  $M_D$  of 7.5–10 TeV/ $c^2$ .

### Experiments at the CERN Super Proton Synchrotron

#### COMPASS

In 2018, the COMPASS collaboration performed an additional data taking on the Drell–Yan measurements program using a polarized hydrogen target and a pion beam with energy 160 GeV.

The  $K^-$  over  $K^+$  multiplicity ratio was measured in deep-inelastic scattering, for the first time for kaons carrying a large  $z$  fraction of the virtual-photon energy [11]. The data were obtained by the COMPASS collaboration using a 160 GeV muon beam and an isoscalar  ${}^6\text{LiD}$  target. Kaons are identified in the momentum range from 12 to 40 GeV/ $c$ , thereby restricting the range in Bjorken- $x$  to  $0.01 < x < 0.40$ . The  $z$ -dependence of the multiplicity ratio is studied for  $z > 0.75$  (Figs. 9 and 10). For large  $z$  values,  $z > 0.8$ , the results contradict expectations obtained using the formalism of (next-to-) leading order perturbative quantum chromodynamics. This may imply that cross-section factorization or/and universality of (kaon) fragmenta-

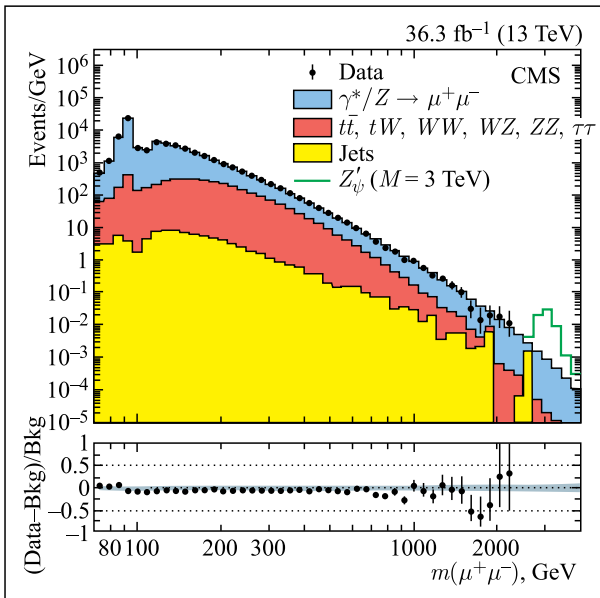


Fig. 7. The invariant mass spectrum of dimuon events. The data of 2016 at 13 TeV are used. The points with error bars represent the observed yield. The histograms represent the expectations from the SM processes

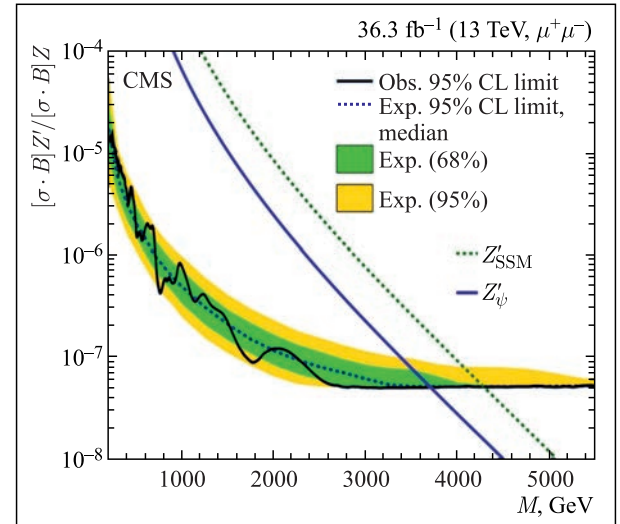


Fig. 8. The upper limits at 95% CL on the product of production cross section and branching fraction for a spin 1 resonance, relative to the product of production cross section and branching fraction of a  $Z$  boson, for the dimuon channel. The shaded bands correspond to the 68 and 95% quantiles for the expected limits. Theoretical predictions for the spin 1  $Z'_{\text{SSM}}$  and  $Z'_{\psi}$  resonances are shown for comparison



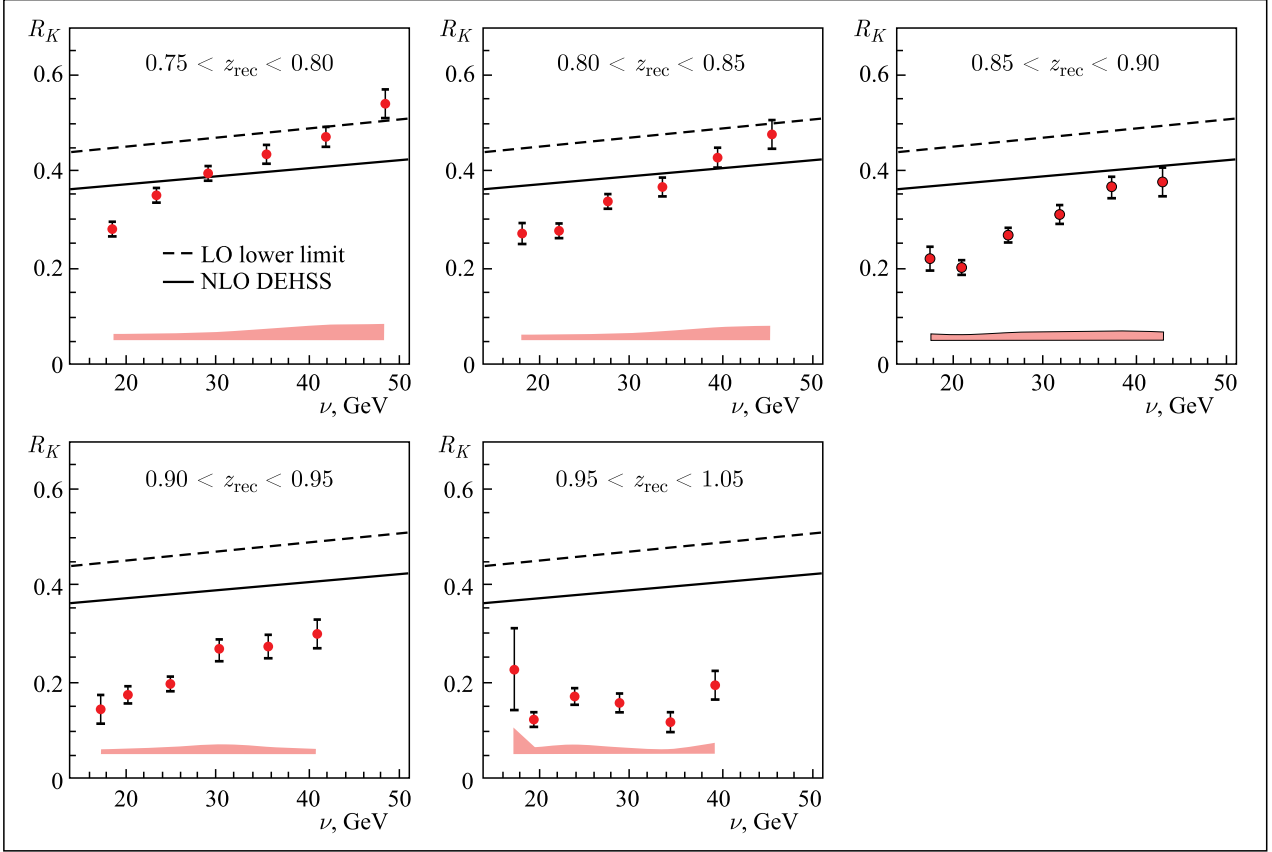


Fig. 9. The  $K^-/K^+$  multiplicity ratio as a function of  $\nu$  in bins of  $z$ , shown for the first bin in  $x$ . QCD predictions are given in solid and dashed lines

tion functions do not hold. Our studies suggest that within this formalism an additional correction may be required, which takes into account the phase space available for hadronization.

For the first time, COMPASS has performed the measurements of exclusive single-photon muoproduction on the proton using 160 GeV/c polarized  $\mu^+$  and  $\mu^-$  beams of the CERN SPS impinging on a liquid hydrogen target. One has determined the dependence of the average of the measured  $\mu^+$  and  $\mu^-$  cross sections for deeply virtual Compton scattering on the squared four-momentum transfer  $t$  from the initial to the final proton. The slope  $B$  of the  $t$ -dependence is fitted with a single exponential function for range 0.1–2 (GeV/c) $^2$ . This result can be converted into an average transverse extension of partons in the proton, for the average virtuality of the photon  $\langle Q^2 \rangle = 1.8$  (GeV/c) $^2$  and the average value of the Bjorken variable equal to  $x_{Bj} = 0.056$  [12].

### NA61/SHINE

In 2018, NA61/SHINE detected the first preliminary indication of critical point observation (Fig. 11). Intermittency signal in protons is expected to increase close to the critical point. At the critical point, a local power law dependence of fluctuations is expected. Preliminary results from the data analysis of Be + Be and Ar + Sc collisions could be the first possible evidence of

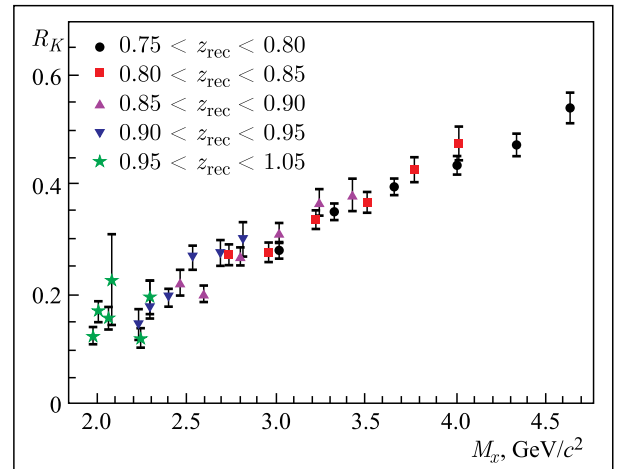


Fig. 10. The  $K^-/K^+$  multiplicity ratio presented as a function of  $x$

critical point at Ar + Sc, while there is no signal in Be + Be data.

### NA62

The search for heavy neutral lepton production in  $K^+$  decays has been performed on the basis of NA62 data collected in 2015 [13]. Upper limits in the range from  $10^{-7}$  to  $10^{-6}$  have been set on the squared mixing matrix element  $|U_{e4}|^2$  and  $|U_{\mu 4}|^2$  for heavy neutrino masses in the ranges 170–448 MeV/c $^2$  and 250–373 MeV/c $^2$ , respectively.

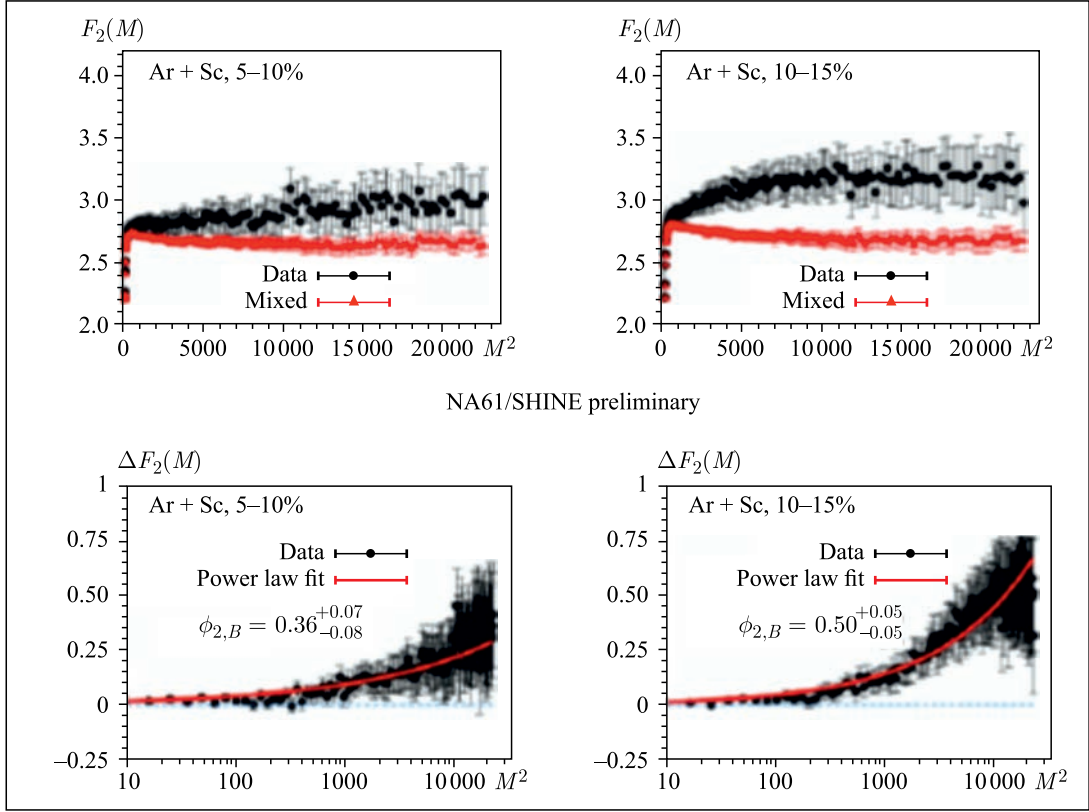


Fig. 11. Top: factorial moments  $F_2(M)$  of identified protons in Ar + Sc collisions at 150A GeV/c for data (black) and mixed events (red). Bottom: background subtracted factorial moment  $\Delta F_2(M)$  exhibits a power law behavior predicted for the systems being in the vicinity to the critical point. This could be the first evidence of critical point signal in the NA61/SHINE

The final paper on the  $K_{e3}$  and  $K_{\mu 3}$  semileptonic decays form factors based on the NA48/2 data is published [14]. A measurement of the form factors of charged kaon semileptonic decays is presented, based on  $4.4 \cdot 10^6$   $K_{e3}$  and  $2.3 \cdot 10^6$   $K_{\mu 3}$  decays collected in 2004 by the NA48/2 experiment. The results are obtained with the improved precision in comparison to earlier measurements. The combination of measurements in both semileptonic modes is also presented.

The final paper on the results of the NA48/2 analysis of the rare decay  $K^\pm \rightarrow \pi^\pm \pi^0 e^+ e^-$ , which had not been observed earlier, was published [15]. Results are based on  $1.7 \cdot 10^{11}$   $K_{ch}$  decays recorded in 2003–2004. A sample of 4919 candidates with 4.9% background contamination allows determining the branching ratio  $BR = (4.24 \pm 0.14) \cdot 10^{-6}$ . The study of the kinematic space shows the evidence for a structure-dependent contribution in agreement with predictions based on chiral perturbation theory (ChPT). Several  $P$ - and  $CP$ -violating asymmetries are also evaluated.

The first NA62 result on the search for  $K^+ \rightarrow \pi^+ \nu \bar{\nu}$  decay based on small subsample of the data collected in 2016 (corresponding to  $1.21 \cdot 10^{11}$   $K^+$  decays) has been published [16] (Fig. 12). The single event sensitivity is  $3.15 \cdot 10^{-10}$  which corresponds to 0.267 Standard Model events. One signal candidate is observed, while the expected background is 0.152 events.

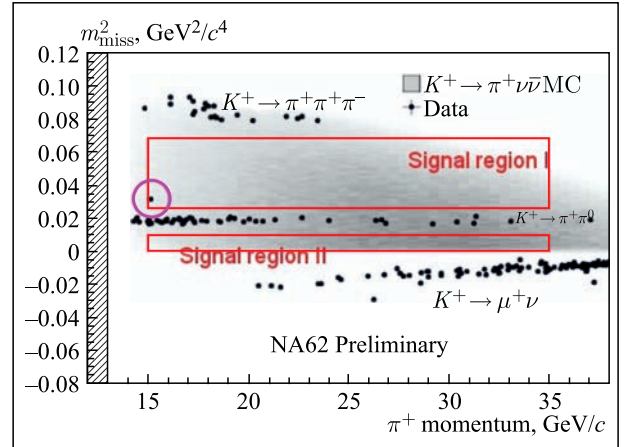


Fig. 12. The first NA62 result on the search for  $K^+ \rightarrow \pi^+ \nu \bar{\nu}$  decay based on small subsample of the data collected in 2016 (corresponding to  $1.21 \cdot 10^{11}$   $K^+$  decays)

The analysis of NA48/2 data in order to investigate the rare decay  $K_{\mu 4}^{00}$ , which has never been observed earlier, is in progress. The events selection for background suppression is developed, the first estimation of branching fraction is in agreement with the available theoretical ChPT prediction.

#### NA64

The main objective of the NA64 experiment is the search for physics beyond the SM, namely, the search

for a light dark photon ( $A'$ ) and other signs of the dark sector.

In 2018, during two runs at the SPS CERN channel, a test run (April 2018) and a data taking one (May–June 2018), six stations of straw detectors (12 double-layer cameras with the size of  $200 \times 200$  mm) were tested and functioned successfully. JINR staff took part in the installation and dismantling of the equipment, maintenance of straw detectors as experts, work in data taking shifts and on-line analysis of the collected data. During the run,  $2 \cdot 10^{11}$  events were collected in the invisible mode and  $3 \cdot 10^{10}$  in the visible one, data analysis goes on.

In 2018, the collaboration completed the analysis, and the data of 2016 and 2017 on the search for a signal of the dark photon in the invisible decay mode were published. Summary statistics of them amounted to  $\sim 10^{11}$ , but no candidate signal that corresponds to the signature of a dark photon was detected [17].

In 2017 the run was partially devoted to the search for a new hypothetical  $X$  boson with the mass of 16.7 MeV, the existence of which could explain the result on the anomalous production of  $e^+e^-$  pairs in the decay of the excited state of  ${}^8\text{Be}^*$  obtained in the ATOMKI experiment,  $5.4 \cdot 10^{10}$  events were taken. The hypothetical boson was not detected, the data obtained allowed to significantly increase the constraint on the probability of its production, complementing the results of other research groups [18] (Fig. 13).

In 2018, the experiment got a permanent experimental zone at CERN on the H4 channel, preparatory works on its arrangement were started.

### Experiments at the Relativistic Heavy Ion Collider, BNL

#### STAR

In 2018, the STAR collaboration reported a new physics phenomenon which had been predicted by the JINR group.

- To study the chiral magnetic effect, a run was conducted and statistics was collected on the isobar nuclei Zr-96 and Ru-96 at the energy of 200 GeV.

## REFERENCES

1. *Sidorin A. et al.* Status of the Nuclotron // Proc. of RuPAC2018, Protvino, Russia, 2018. P. 49–51.
2. *Baranov D. et al.* First Results from BM@N Technical Run with Deuteron Beam // Phys. Part. Nucl. Lett. 2018. V. 15, No. 2. P. 148–156.
3. *SPD Team.* Conceptual and Technical Design of the Spin Physics Detector (SPD) at the NICA Collider, October 2018; <http://indico.jinr.ru/conference/Display.py?confId=665>.
4. *Avdeyev S.P., Karcz W., Kirakosyan V.V., Rukoyatkin P.A., Stegaylov V.I., Oeschler H., Botvina A.S.* Time Scale of the Thermal Multifragmentation in

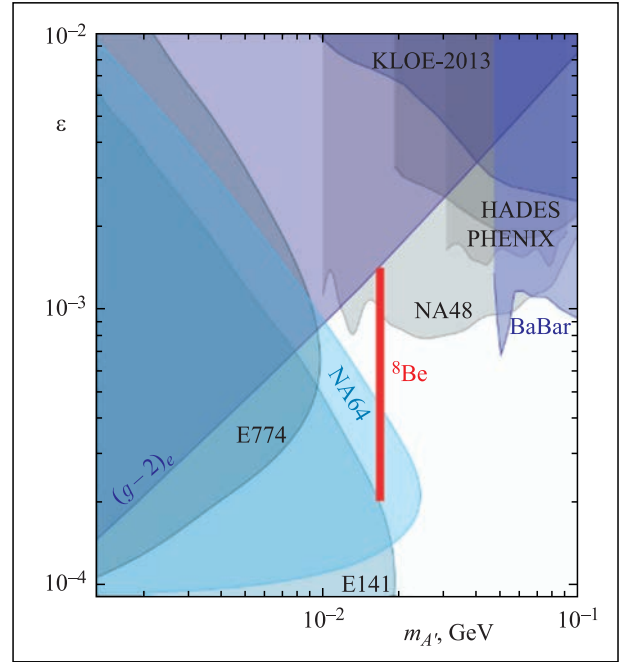


Fig. 13. The 90% CL exclusion areas in the  $(m_{A'}, \epsilon)$  plane from the NA64 (blue area). For the mass of 16.7 MeV, the region excluded by NA64 is  $1.3 \cdot 10^{-4} < \epsilon < 4.2 \cdot 10^{-4}$ . The allowed range of  $\epsilon$  explaining the  ${}^8\text{Be}^*$  anomaly (red area) and constraints from other experiments are shown

- Earlier (in 2017), the global polarization of lambda in the energy range of 10–60 GeV had been detected. In 2018, new data on the presence of global polarization of  $\Lambda$  and  $\bar{\Lambda}$  at maximum RHIC energy of 200 GeV were published. A special area of research interests of the Dubna group in the STAR experiment is the study of global polarization in the range of NICA energies in the collider mode and the corresponding measurements with a fixed target in the STAR experiment.

- One of the new results is the study of the antiproton correlation function. These are direct measurements of antinucleon interactions. New results on  $pp$  and  $p\bar{p}$  at 39 GeV were presented at the international conference “Quark Matter 2018” (Venice, Italy).

${}^4\text{He}(4 \text{ GeV}) + \text{Au}$  Collisions // Bull. Russ. Acad. Sci.: Phys. 2018. V. 82, No. 6. P. 711.

5. *Janek M. et al.* Calibration Procedure of the  $\Delta E - E$  Detectors for  $dp$  Breakup Investigation at Nuclotron // Phys. Part. Nucl. Lett. 2018. V. 15. P. 76.
6. *Acharya S. et al. (ALICE Collab.).* Azimuthally Differential Pion Femtoscopy Relative to the Third Harmonic Event Plane in Pb–Pb Collisions at  $(s_{NN})^{1/2} = 2.78 \text{ TeV}$  // Phys. Lett. B. 2018. V. 785. P. 320–331.
7. *Acharya S. et al. (ALICE Collab.).* Inclusive  $J/\psi$  Production in Xe–Xe Collisions at  $(s_{NN})^{1/2} =$

- 5.02 TeV // Phys. Lett. B. 2018. V. 785. P. 419–428.
8. *The ATLAS Collab.* Observation of  $H \rightarrow bb$  Decays and  $VH$  Production with the ATLAS Detector // Phys. Lett. B. 2018. V. 786. P. 59; DOI:10.1016/j.physletb.2018.09.013; ATLAS CONF Note: ATLAS-CONF-2018-036; <https://cds.cern.ch/record/2630338/files/ATLAS-CONF-2018-036.pdf>.
  9. *Sirunyan A. M. et al. (CMS Collab.)*. Search for High-Mass Resonances in Dilepton Final States in Proton–Proton Collisions at 13 TeV // JHEP. 2018. V. 1806. P. 120; arXiv:1803.06292.
  10. *Abbiendi G. et al.* Performance of High- $p_t$  Muons Collected with CMS at 13 TeV during Proton–Proton Collisions. CMS AN-2018/008.
  11. *COMPASS Collab.*  $K^-$  over  $K^+$  Multiplicity Ratio for Kaons Produced in DIS with a Large Fraction of the Virtual-Photon Energy // Phys. Lett. B. 2018. V. 786. P. 390.
  12. *COMPASS Collab.* Transverse Extension of Partons in the Proton Probed by Deeply Virtual Compton Scattering. CERN-EP/2018-016; Phys. Lett. B (submitted).
  13. *Cortina Gil E. et al. (NA62 Collab.)*. Search for Heavy Neutral Lepton Production in  $K^+$  Decays // Phys. Lett. B. 2018. V. 778. P. 137.
  14. *Batley J. R. et al. (NA48/2 Collab.)*. Measurement of the Form Factors of Charged Kaon Semileptonic Decays // JHEP. 2018. V. 1810. P. 150.
  15. *Batley J. R. et al. (NA48/2 Collab.)*. First Observation and Study of the  $K^\pm \rightarrow \pi^\pm \pi^0 e^+ e^-$  Decay. arXiv:1809.02873 [hep-ex]; Phys. Lett. B (submitted).
  16. *Cortina Gil E. et al. (NA62 Collab.)*. First Search for  $K^+ \rightarrow \pi^+ \nu \nu$  Using the Decay-in-Flight Technique. CERN-EP-2018-314.
  17. *Banerjee D. et al. (NA64 Collab.)*. Search for Vector Mediator of Dark Matter Production in Invisible Decay Mode // Phys. Rev. D. 2018. V. 97. P. 072002.
  18. *Banerjee D. et al. (NA64 Collab.)*. Search for a New  $X(16.7)$  Boson and Dark Photons in the NA64 Experiment at CERN // Phys. Rev. Lett. 2018. V. 120. P. 231802.